Molecular Astrophysics 3–4 (2016) 16–20

Contents lists available at ScienceDirect

Molecular Astrophysics

journal homepage: www.elsevier.com/locate/molap

High resolution absorption cross sections for propylene in the 3 μm region at high temperatures

Eric M. Buzan*, Robert J. Hargreaves[1], Peter F. Bernath

Department of Chemistry and Biochemistry, Old Dominion University, 4541 Hampton Boulevard, Norfolk, VA 23529, USA

ARTICLE INFO

Article history:
Received 25 April 2016
Revised 7 June 2016
Accepted 14 June 2016
Available online 25 June 2016

Keywords:
Infrared
High resolution
Absorption cross sections
Planetary atmospheres
Exoplanets

ABSTRACT

High resolution infrared spectra in the 3 μm region for propylene (C_3H_6) were recorded at temperatures up to 700 K. Measurements were taken using a Fourier transform infrared spectrometer at a resolution of 0.005 cm^{-1} using a quartz cell inside a tube furnace. Calculated cross sections were calibrated against composite spectra from the Pacific Northwest National Laboratory. These cross sections are provided with this work and will find use in remote sensing and combustion monitoring.

Introduction

Propylene, also known as propene, is a small unsaturated hydrocarbon with the formula C_3H_6. It is the second most important compound in the petrochemical industry behind ethylene (C_2H_4) and is used in the production of many products, especially polypropylene ($(C_3H_6)_n$). It is present in the Earth's atmosphere at a concentration of around 10 ppt (Helmig et al. 2014), and has both natural and anthropogenic sources including biomass burning (Blake et al. 1994), incomplete fossil fuel combustion (Guo et al. 2011), and hydrocarbon cracking (Rahimi & Karimzadeh 2011).

Propylene is also an important molecule in astrochemistry due to its abundance in certain astronomical objects. Rotational line transitions were first observed in the dark cloud TMC-1 using the IRAM 30 m radio telescope, and its abundance was comparable to that of other hydrocarbons such as c-C_3H_2. (Marcelino et al. 2007). In response, several mechanisms for the formation of propylene in interstellar space have been proposed. An early hypothesized mechanism was from the dissociative recombination of $C_3H_7^+$, itself formed from several ion-molecule reactions (Marcelino et al. 2007). However, recent ab initio calculations dispute whether this mechanism is fast enough to produce observed abundances (Lin et al. 2013) and that improved grain surface chemistry models are needed (Agúndez et al. 2015). It has also been proposed propylene forms in gas clouds created by rapid sublimation of ice mantles on dust grains (Rawlings et al. 2013). Given the relatively large abundance C_3H_6, the chemical pathways are not fully understood to produce such a large molecule with the observed abundances and more work is needed.

Propylene has also been observed with the Composite Infrared Spectrometer (CIRS) on Cassini in the atmosphere of Titan (Nixon et al. 2013), a moon rich in hydrocarbon species (Cui et al. 2009). Its discovery filled a gap in the list of C_3-hydrocarbons observed in the atmosphere of Titan (Li et al. 2015). Its abundance is notable for being lower than both propane (C_3H_8) and propyne (C_3H_4); like other hydrocarbons in Titan, the alkene (propylene) is more susceptible to photolysis and chemical attack than the more abundant alkyne (propyne).

Propylene is also an important species in some high temperature systems. It is a major component of liquefied petroleum gas and is an intermediate in the combustion of larger hydrocarbons (Burke et al. 2014; Chrystie et al. 2015). Although it has not yet been detected, propylene is expected to be present in the atmosphere of hot exoplanets, and atmospheric models of these bodies have begun incorporating propylene (Venot et al. 2015). While its abundance is not expected to be high, its inclusion is important as it is present in the heavily congested 3 μm region.

Propylene has C_S symmetry and 21 vibrational modes, all of which are infrared active. The infrared and microwave spectrum of propylene has been studied previously by several groups. One of the earliest observations made assignments of all of the fundamental bands and many overtone and combination bands in the 400–6200 cm^{-1} (Lord & Venkateswarlu 1953). The microwave spectrum

* Corresponding author.
E-mail address: ebuzan@odu.edu (E.M. Buzan).
[1] Present address: Atmospheric, Oceanic and Planetary Physics, University of Oxford, Clarendon Laboratory, Parks Road, Oxford, OX1 3PU, UK.

http://dx.doi.org/10.1016/j.molap.2016.06.001
2405-6758/

Table 1
Absorption bands in the 3 μm region.

Band	Band center (cm^{-1})	Symmetry	Description	Source
ν_1	3091.62	a'	CH_2 asymmetric stretch	(Es-sebbar et al. 2014)
ν_2	3012.8	a'	CH stretch	(Lord & Venkateswarlu 1953)
ν_3	2991.03	a'	CH_2 symmetric stretch	(Es-sebbar et al. 2014)
ν_{15}	2954.30	a″	CH_3 asymmetric stretch	(Es-sebbar et al. 2014)
ν_4	2973.0	a'	CH_3 asymmetric stretch	(Silvi et al. 1973)
ν_5	2931.46	a'	CH_3 symmetric stretch	(Es-sebbar et al. 2014)
$2\nu_{16}$	2868.2	a'	CH_3 asymmetric in-plane bending	(Silvi et al. 1973)
$\nu_{10}+\nu_{16}$	2736	a″		(Lord & Venkateswarlu 1953)

of propylene and one isotopologue have been used to determine the structure of the three carbon chain and energy barriers to internal rotation (Lide & Mann 1957). Later, microwave spectra of five additional isotopologues were used to calculate a full structure (Lide & Christensen 1961). Force constants for several modes have been derived from spectra of the 400 and 2000 cm^{-1} region (Silvi et al. 1973). The far infrared spectrum of propylene (80–370 cm^{-1}) has been observed at moderate resolution, resulting in the assignment of the methyl torsional fundamental at 189 cm^{-1} and two hot bands (Durig et al. 1989). Jet spectra have been used to resolve the rotational structure of the ν_{18} (991 cm^{-1}) and ν_{19} (913 cm^{-1}) bands (Lafferty et al. 2006).

In certain regions, the spectrum of propylene becomes heavily congested due to the overlap of several bands as shown in Table 1, making individual line assignments very difficult. Instead, recent high-resolution studies have reported cross sections. The database of infrared spectra maintained by the Pacific Northwest National Laboratory (PNNL) includes absorption cross sections of propylene at 278, 298 and 323 K. These spectra are a composite of measurements made at different pressures and are reported at a spectral resolution of 0.112 cm^{-1} (Sharpe et al. 2004). More recently, spectra were measured of propylene in the range 400–6500 cm^{-1} at a resolution of 0.08 cm^{-1} at temperatures between 298 K and 460 K to determine the cross sections of several regions (Es-sebbar et al. 2014).

However, no studies have been made at higher temperatures or higher resolution than those of Es-sebbar et al. Higher temperatures are needed for the study of combustion chemistry and reaction pathways as well as for hot exoplanets. At higher resolution spectral features are better resolved, improving the accuracy of cross section measurements. This paper reports high-resolution infrared spectra and cross sections of propylene in the region 2500 cm^{-1} to 3200 cm^{-1} from 296 K to 700 K. The cross sections are then calibrated against those from the PNNL database to correct for errors in the experimental pressure.

Material and methods

Several transmittance spectra of propylene (Airgas, 99.99%) were acquired in the 3 μm region covering the bands listed in Table 1 at a resolution of 0.005 cm^{-1}. The Bruker definition of resolution of 0.9 divided by the maximum optical path difference is used. Measurements were made at 296 K (i.e., room temperature) and from 400 K to 700 K at 100 K intervals. Several low-resolution test measurements were made at different pressures at each temperature. One pressure was selected for each temperature for high-resolution measurements; this pressure was chosen to give a good absorption depth that was comparable for each temperature, but not enough to saturate any lines. A figure showing the transmission at each temperature are given in the Supplementary Material. At most temperatures, two spectra were measured: an absorption spectrum of propylene (A_{ab}) and background (A_{ref}) from which the transmission is calculated (i.e., $T = A_{ab}/A_{ref}$). At 600 K and 700 K, emission from propylene becomes significant and has to be accounted for. Therefore two additional spectra, propylene emission (B_{em}) and background emission, (B_{ref}) are acquired. These spectra are subtracted from the absorption spectrum as

$$\tau = \frac{A_{ab} - B_{em}}{A_{ref} - B_{ref}}. \quad (1)$$

Each spectrum is an average of 600 scans (at 296 K), 300 scans (at 400–500 K), or 150 scans (at 600–700 K) to improve the signal-to-noise ratio.

This method has previously been used to account for the emission component in high temperature methane (Hargreaves et al. 2015a), ethane (Hargreaves et al. 2015b), and propane (Beale et al. 2016) spectra.

The instrumental setup is similar to that used for studies of other hydrocarbons (Hargreaves et al. 2015a,2015b; Harrison et al. 2012). The spectra were obtained using a Bruker IFS 125 HR Fourier transform spectrometer with an InSb detector and a CaF_2 beamsplitter. The sample was contained in a 0.5 m quartz cell placed inside of a tube furnace. The cell is built such that the entire sample chamber is contained within the heated portion of the furnace. For absorption measurements, a glowbar was used as a broadband light source. The full experimental conditions are listed in Table 2.

Absorption cross sections as a function of wavenumber were calculated using the equation

$$\sigma(\nu) = -\xi \frac{10^4 k_B T}{Pl} \ln \tau(\nu) \quad (2)$$

where k_B is the Boltzmann constant, T is the temperature (K), P is the pressure (Pa), l is the path length (m), τ is the transmittance at a given wavenumber, and ξ is an empirical normalization factor calculated by comparison to the spectra from the PNNL database. These composite spectra were selected to perform the correction because of their high quality due to the use of several pressure/path lengths. Initially, $\xi = 1$, and the cross sections are integrated over the range 2650–3300 cm^{-1} to give an integrated cross section in units of cm $molecule^{-1}$. The three PNNL spectra, measured at 278, 298 and 323 K, are also integrated in this manner to give values of 1.6975×10^{-17}, 1.6987×10^{-17}, and 1.6961×10^{-17} cm/molecule, respectively. The mean value, 1.6975×10^{-17} cm/molecule was used for calibration. The value of ξ in Eq. (1) is adjusted to set our integrated cross section equal to that of the mean PNNL integrated cross section.

Results and discussion

The propylene absorption cross sections are displayed in Fig. 1. At lower temperatures, individual lines for several bands are visible including ν_1 (3091 cm^{-1}), ν_{15} (2954 cm^{-1}), ν_5 (2932 cm^{-1}), $2\nu_{16}$ (2868 cm^{-1}), and $\nu_{10}+\nu_{16}$ (2737 cm^{-1}). As the temperature increases, the peak absorption of each band decreases as the lines broaden. The sharp features clearly visible at low temperatures can still be seen but become less pronounced. Fig. 2 demonstrate this effect on the entire $2\nu_{16}$ band and individual lines in its P branch;

Table 2
Summary of experimental conditions.

Parameter	Value
Temperature	296, 400, 500, 600, 700 K
Spectral range	1800–5600 cm^{-1}
Resolution	0.005 cm^{-1}
IR source	Glowbar
Detector	InSb
Beam splitter	CaF_2
Windows	CaF_2 (lens, spectrometer) Quartz (cell)
Filter	Germanium
Apodization	Norton-Beer weak
Scans per spectrum	296 K: 600 scans 400–500 K : 300 scans 600–700 K: 150 scans

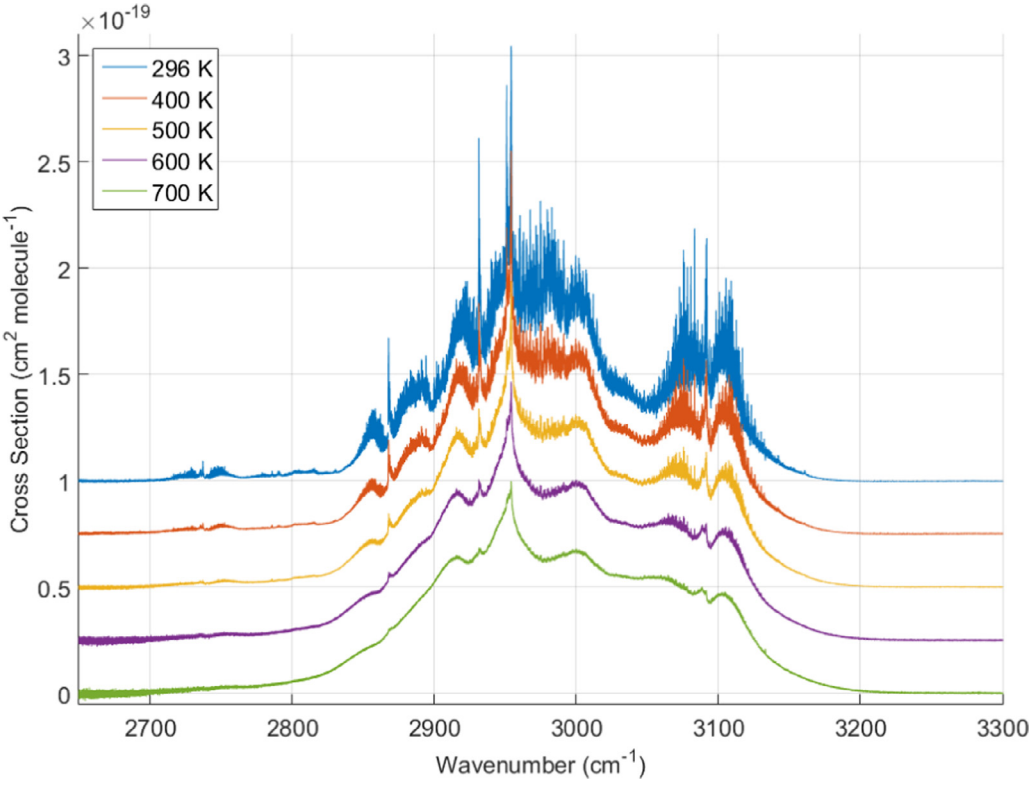

Fig. 1. Propylene cross sections for the 3 μm region at a resolution of 0.005 cm^{-1}. Each temperature is offset by 2.5×10^{-20} cm^2 mol^{-1}.

Table 3
Uncalibrated integrated cross sections and normalization factors .

Temperature (K)	Integrated cross section (cm mol^{-1})	Normalization factor ξ	Effective pressure (Torr)
296	1.640×10^{-17}	1.035	4.86
400	1.687×10^{-17}	1.006	6.56
500	1.663×10^{-17}	1.020	7.99
600	1.685×10^{-17}	1.007	9.53
700	1.620×10^{-17}	1.048	10.54

the detailed structure is reduced to a nearly smooth slope. The integrated region was chosen to cover an isolated set of bands. Several previous studies have shown that integrated cross sections over an isolated region are temperature independent (Es-sebbar et al. 2014; Hargreaves et al. 2015b). This behavior was also seen with propylene and is shown in Table 3.

The calibrated absorption cross sections are provided in the Supplementary Material.

Several sources of systematic error are present in the absorption cross sections. Error in temperature is estimated at 1%. The pressure error is estimated to be 2% due to fluctuations of the measured pressure at this magnitude from the beginning to the end of a measurement. The pressure reported is that at the beginning of the measurement and the pressure increased very slowly with time because of a very small air leak. Photometric error was estimated at 2% and can be attributed to drifts in the light source brightness, detector and electronics response. The pathlength error is at 0.2% and was determined by direct measurement. We estimate the overall uncertainty to be approximately 4%. The continuum signal-to-noise ratios in the final transmission spectra ranged from 1167 at 296 K to 655 at 700 K, so that the systematic error is the dominant source of error in the cross sections.

The normalization factors given in Table 3 correct for systematic error in the spectra under the assumption that pressure is the

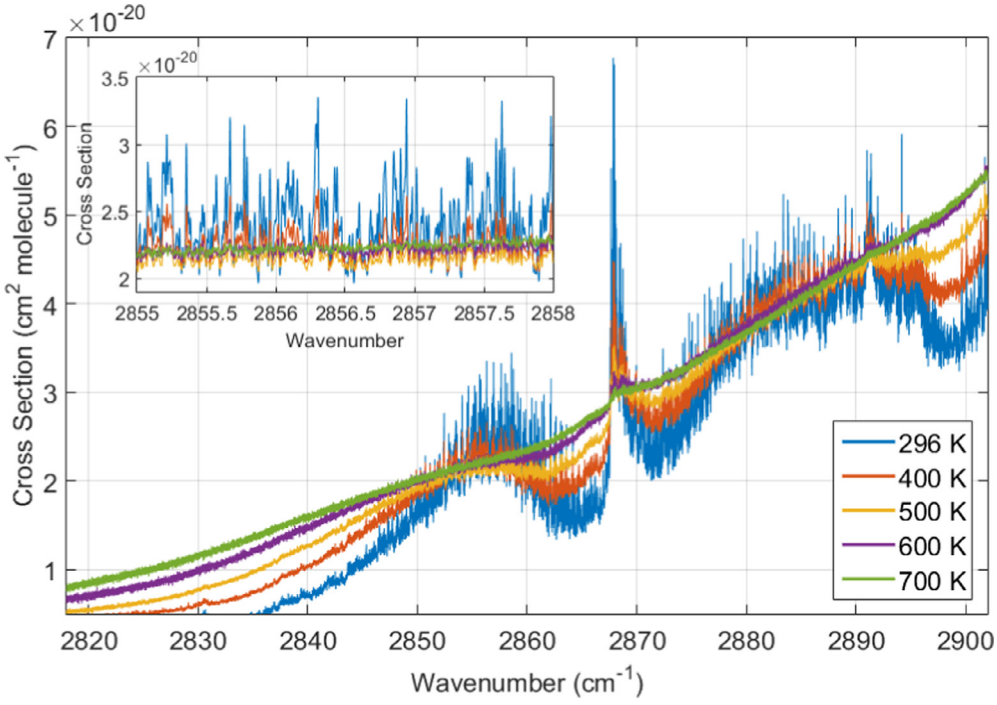

Fig. 2. The $2\nu_{16}$ band of propylene. The effect of temperature on the structure of the band is visible. The inset figure shows a section of the P branch.

Table 4
Comparison of room temperature integrated cross sections for the region 2500–3200 cm^{-1}. %difference = $(S - S_{this\ work})/S_{this\ work}$.

Source	Resolution (cm^{-1})	Integrated Cross Section ($cm\ mol^{-1}$)	% difference from this work
This work	0.005	1.639×10^{-17}	–
(Es-sebbar et al. 2014)	0.08	1.658×10^{-17}	1.2%
PNNL (Sharpe et al. 2004)	0.11	1.698×10^{-17}	3.4%
(NIST Mass Spec Data Center 2016)	2	1.717×10^{-17}	4.8%

only source of this error, though this is obviously not true. Combing the normalization factor with the measured pressure gives an effective pressure that allows the integrated cross section of the PNNL spectra to be replicated by this work. The smallest corrections were applied to the 400, 500 and 600 K measurements with an error of no more than 2%. Nonetheless, all integrated cross sections in this work agree with PNNL to less than 5% and so have similar normalization factors.

To independently verify our absorption cross sections, we compare them to those measured by Es-sebbar et al. (2014). Although these spectra were measured at different temperatures and at a higher resolution, 0.005 cm^{-1} versus 0.08 cm^{-1}, neither of these should have a large effect on the cross sections integrated over the same wavenumber region. At 296 K, Es-sebbar et al. reports an integrated cross section of 1.658×10^{-17} $cm\ mol^{-1}$ in the region 2500–3200 cm^{1}.This is only a 1.2% difference from the 296 K measurement of 1.639×10^{-17} $cm\ mol^{-1}$ in this work. Other measurements were not taken at the same temperatures, but all integrated cross sections from both data sets agree to within 5%. This comparison is summarized in Table 4 along with a comparison to PNNL and a spectrum from the National Institute of Standards and Technology (NIST) database (NIST Mass Spec Data Center 2016).

Fig. 3 shows the benefits of making cross-section measurements at high resolution. In previous work, such as that of Es-sebbar et al., individual lines are not resolved, while in this work, the structure of these lines is clearly visible.

Beyond the spectra reported here, measurements were made at 800 K. Thermal decomposition of propylene was observed from a decreasing signal and the appearance of strong absorption features attributed to methane. Accurate absorption cross sections of propylene could therefore not be provided at 800 K.

The spectra and cross sections presented here are expected to assist with the detection of propylene and similar hydrocarbons in astronomical objects such as hot Jupiters and in combustion environments. As a low temperature example, recent observations of propylene in Titan's atmosphere (Nixon et al. 2013) were achieved by observing the residual spectrum from CIRS after removing other hydrocarbons such as propane using high-resolution cross sections. Recent high-resolution spectra of propane (Sung et al. 2013) were crucial for this detection. Improved profiles of propane over Titan were also obtained by subtracting several hydrocarbon species (Nixon et al. 2009). In this study, propylene was not used, but adding the propylene cross section would help to improve propane measurements by reducing the residuals. In addition, combustion environments such as those in automotive engines contain a variety of hydrocarbon species that can exhibit non-linear behavior between absorption and hydrocarbon density (Grosch et al. 2011). High quality spectra at high temperature of the gases at high temperature are crucial for properly quantifying their concentration.

Conclusion

This paper presents spectra of the 2500–3200 cm^{-1} region of propylene measured at both higher resolution and higher temperatures than previous measurements. These spectra produce improved cross section of the 3 μm region of propylene (including the ν_1, ν_{15}, ν_5, $2\nu_{16}$, and $\nu_{10}+\nu_{16}$ bands) and confirm the temperature independence of the integrated cross section in this region.

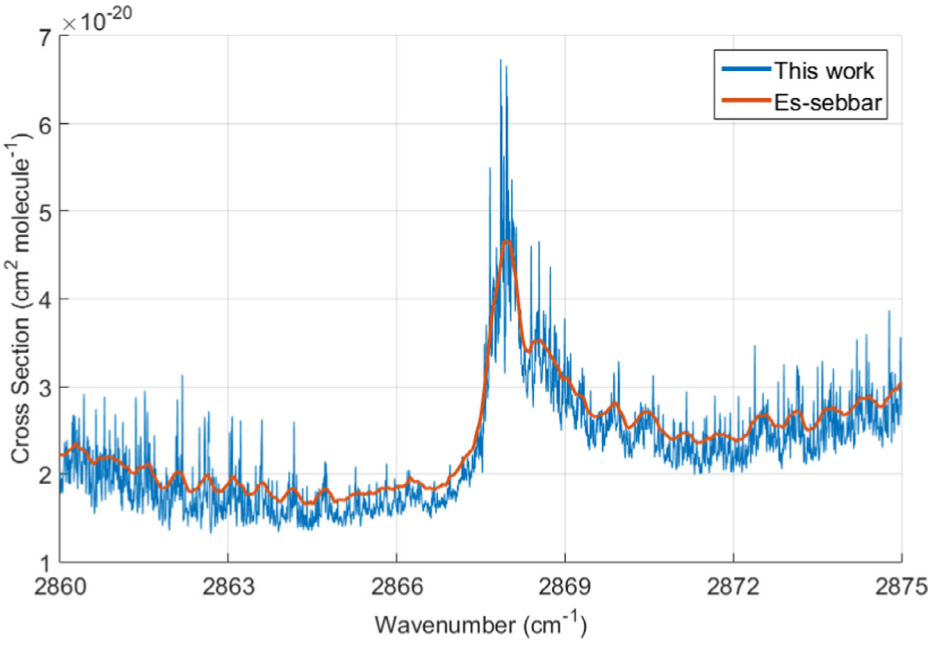

Fig. 3. Comparison of this work and that of Es-sebbar et al. for the $2\nu_{16}$ Q branch.

These data are expected to help with the detection of propylene in astronomical objects and aid experiments in combustion chemistry.

Acknowledgments

Support was provided by the NASA Planetary Atmospheres program.

Supplementary materials

Supplementary material associated with this article can be found, in the online version, at doi:10.1016/j.molap.2016.06.001.

References

Agúndez, M., Cernicharo, J., & Guélin, M. 2015, Astron. Astrophys., 577, L5. doi:10.1051/0004-6361/201526317.
Beale, C.A., Hargreaves, R.J., & Bernath, P.F. 2016, J. Quant. Spectrosc. Radiat. Transf, 182, 219–224. doi:10.1016/j.jqsrt.2016.06.006.
Blake, D.R., Smith, T.W., Chen, T.-Y., Whipple, W.J., & Rowland, F.S. 1994, J. Geophys. Res., 99, 1699. doi:10.1029/93JD02598.
Burke, S.M., Metcalfe, W., Herbinet, O., Battin-Leclerc, F., Haas, F.M., Santner, J., Dryer, F.L., & Curran, H.J. 2014, Combust. Flame, 161, 2765–2784. doi:10.1016/j.combustflame.2014.05.010.
Chrystie, R.S.M., Nasir, E.F., & Farooq, A. 2015, Appl. Phys. B, 120, 317–327. doi:10.1007/s00340-015-6139-4.
Cui, J., Yelle, R.V., Vuitton, V., Waite, J.H., Kasprzak, W.T., Gell, D.A., Niemann, H.B., Müller-Wodarg, I.C.F., Borggren, N., Fletcher, G.G., Patrick, E.L., Raaen, E., & Magee, B.A. 2009, Icarus, 200, 581–615. doi:10.1016/j.icarus.2008.12.005.
Durig, J.R., Guirgis, G.A., & Bell, S. 1989, J. Phys. Chem., 93, 3487–3491. doi:10.1021/j100346a026.
Es-sebbar, E., Alrefae, M., & Farooq, A. 2014, J. Quant. Spectrosc. Radiat. Transf., 133, 559–569. doi:10.1016/j.jqsrt.2013.09.019.
Grosch, A., Beushausen, V., Wackerbarth, H., Thiele, O., Berg, T., & Grzeszik, R. 2011, J. Quant. Spectrosc. Radiat. Transf., 112, 994–1004. doi:10.1016/j.jqsrt.2010.11.016.
Guo, H., Zou, S.C., Tsai, W.Y., Chan, L.Y., & Blake, D.R. 2011, Atmos. Environ., 45, 2711–2721. doi:10.1016/j.atmosenv.2011.02.053.
Hargreaves, R.J., Bernath, P.F., Bailey, J., & Dulick, M. 2015a, Astrophys. J., 813(12). doi:10.1088/0004-637X/813/1/12.
Hargreaves, R.J., Buzan, E., Dulick, M., & Bernath, P.F. 2015b, Mol. Astrophys., 1, 20–25. doi:10.1016/j.molap.2015.09.001.
Harrison, J.J., Allen, N.D.C., & Bernath, P.F. 2012, J. Quant. Spectrosc. Radiat. Transf., 113, 2189–2196. doi:10.1016/j.jqsrt.2012.07.021.
Helmig, D., Stephens, C.R., Caramore, J., & Hueber, J. 2014, Atmos. Environ., 85, 234–246. doi:10.1016/j.atmosenv.2013.11.021.
Lafferty, W.J., Flaud, J.-M., & Herman, M. 2006, J. Mol. Struct., 780-781, 65–69. doi:10.1016/j.molstruc.2005.03.051.
Li, C., Zhang, X., Gao, P., & Yung, Y. 2015, Astrophys. J., 803, L19. doi:10.1088/2041-8205/803/2/L19.
Lide, D.R. & Christensen, D. 1961, J. Chem. Phys., 35, 1374. doi:10.1063/1.1732055.
Lide, D.R. & Mann, D.E. 1957, J. Chem. Phys., 27, 868. doi:10.1063/1.1743867.
Lin, Z., Talbi, D., Roueff, E., Herbst, E., Wehres, N., Cole, C.A., Yang, Z., Snow, T.P., & Bierbaum, V.M. 2013, Astrophys. J., 765, 80. doi:10.1088/0004-637X/765/2/80.
Lord, R.C. & Venkateswarlu, P. 1953, J. Opt. Soc. Am., 43, 1079. doi:10.1364/JOSA.43.001079.
Marcelino, N., Cernicharo, J., Agúndez, M., Roueff, E., Gerin, M., Martín-Pintado, J., Mauersberger, R., & Thum, C. 2007, Astrophys. J., 665, L127–L130. doi:10.1086/521398.
NIST Mass Spec Data Center 2016. "Infrared Spectra." In Linstrom, P.J. & W.G. Mallard. NIST Chemistry WebBook, NIST Standard Reference Database Number 69 (Gaithersburg, MD: National Institute of Standards and Technology).
Nixon, C.a., Jennings, D.E., Flaud, J.M., Bézard, B., Teanby, N.A., Irwin, P.G.J., Ansty, T.M., Coustenis, A., Vinatier, S., & Flasar, F.M. 2009, Planet. Space Sci., 57, 1573–1585. doi:10.1016/j.pss.2009.06.021.
Nixon, C.A., Jennings, D.E., Bézard, B., Vinatier, S., Teanby, N.A., Sung, K., Ansty, T.M., Irwin, P.G.J., Gorius, N., Cottini, V., Coustenis, A., & Flasar, F.M. 2013, Astrophys. J., 776, L14. doi:10.1088/2041-8205/776/1/L14.
Rahimi, N. & Karimzadeh, R. 2011, Appl. Catal. A Gen., 398, 1–17. doi:10.1016/j.apcata.2011.03.009.
Rawlings, J.M.C., Williams, D.a., Viti, S., & Cecchi-Pestellini, C. 2013, Mon. Not. R. Astron. Soc. Lett., 436, L59–L63. doi:10.1093/mnrasl/slt113.
Sharpe, S.W., Johnson, T.J., Sams, R.L., Chu, P.M., Rhoderick, G.C., & Johnson, P.a. 2004, Appl. Spectrosc., 58, 1452–1461. doi:10.1366/0003702042641281.
Silvi, B., Labarbe, P., & Perchard, J.P. 1973, Acta Part A Mol. Spectrosc., 29, 263–276. doi:10.1016/0584-8539(73)80070-4.
Sung, K., Toon, G.C., Mantz, A.W., & Smith, M.A.H. 2013, Icarus, 226, 1499–1513. doi:10.1016/j.icarus.2013.07.028.
Venot, O., Hébrard, E., Agúndez, M., Decin, L., & Bounaceur, R. 2015, Astron. Astrophys., 577, A33. doi:10.1051/0004-6361/201425311.